PROTEINS: Structure, Function, and Genetics 48:212–219 (2002)

Signal Transduction in the Photoactive Yellow Protein. II. Proton Transfer Initiates Conformational Changes

Gerrit Groenhof,[1] Marc F. Lensink,[2] Herman J. C. Berendsen,[1] Alan E. Mark[1]*
[1]*Department of Biophysical Chemistry, Groningen Biomolecular Sciences and Biotechnology Institute, Rijksuniversiteit Groningen, Groningen, The Netherlands*
[2]*Department of Biochemistry, the University of Oulu, Oulu, Finland*

ABSTRACT **Molecular dynamics simulation techniques, together with *semiempirical* PM3 calculations, have been used to investigate the effect of photoisomerization of the 4-hydroxy-cinnamic acid chromophore on the structural properties of the photoactive yellow protein (PYP) from *Ectothiorodospira halophila*. In this bacteria, exposure to blue light leads to a negative photoactic response. The calculations suggest that the isomerization does not directly destabilize the protein. However, because of the isomerization, a proton transfer from a glutamic acid residue (Glu^{46}) to the phenolate oxygen atom of the chromophore becomes energetically favorable. The proton transfer initiates conformational changes within the protein, which are in turn believed to lead to signaling. Proteins 2002;48:212–219.**

Key words: photoactive yellow protein; signal transduction; proton transfer; molecular dynamics; semiempirical PM3 calculations

INTRODUCTION

Ectothiorodospira halophila, a small salt-tolerant bacterium always moves in directions opposite to blue light gradients to minimize exposure to harmful ultraviolet radiation.[1] A small water-soluble protein, named photoactive yellow protein (PYP) has been proposed to be the primary photoreceptor for this biological process. It contains a 4-hydroxy-cinnamic acid (or *p*-coumaric acid) chromophore covalently bound to a cysteine residue [Cys^{69}; Fig. 1(a) of the previous article[2]].[3] The chromophore is deprotonated and stabilized by a hydrogen-bonding network with nearby residues [Tyr^{42}, Glu^{46}, and Thr^{50}; Fig. 1(b) of the previous article[2]].[4]

On absorption of a blue light photon (λ_{max} = 446 nm), PYP enters a fully reversible photocycle, depicted in Fig. 2 of the previous article.[2] The absorption triggers a fast *trans*-to-*cis* isomerization of the double bond of the chromophore, leading to the red-shifted state (pR).[5,6] During the isomerization, the hydrogen-bonding network remains intact.[7] After the isomerization, the protein partially unfolds over a period of microseconds, leading to the blue-shifted state (pB) in which the unfolding is at a maximum.[8,9] Therefore, this state is believed to be the signaling state of PYP. During the unfolding, the chromophore becomes protonated. One possible explanation for this observation is that a proton is transferred from one of the hydrogen-bonding donors [Fig. 1(b)[2]] to the chromophore and that this transfer induces the unfolding. However, it has also been proposed that the isomerization itself triggers the unfolding and that during this unfolding the chromophore becomes solvent exposed and picks up a proton from there. A third possibility is that a water molecule enters the chromophore cavity during the third stage and that the proton is transferred from one of the hydrogen bond donors to the chromophore via that water molecule. After reaching the blue-shifted state, the chromophore slowly refolds, the chromophore reisomerizes, loses its proton, and the system is restored to its equilibrium state (pG). For a more elaborate introduction to PYP, the reader is referred to our previous paper.[2]

To understand how the absorption of a photon by the chromophore leads to large conformational changes elsewhere in the protein, we performed a number of molecular dynamics (MD) simulation studies on PYP. In an MD simulation, the equations of motion for all atoms in a system are integrated in time.[10,11] This way, one obtains a description of the dynamics of the system at an atomic level. With the current state of computer technology, the maximum timescale that can be reached in a classical simulation of a small protein (~20,000 atoms) is in the order of 10–100 ns. Therefore, MD is limited to relatively fast processes. In PYP, processes take place on many different timescales. For example, the isomerization of the chromophore takes place within nanoseconds, whereas the refolding takes milliseconds.

We examined the first three stages of the photocycle in detail. Work on the first two stages was presented in a previous article. It was shown that the energy barrier for the isomerization of the chromophore is considerably lower in the excited state. Moreover, it was shown that this isomerization takes place with only minimal rearrangements in the protein. In this article, we focus on the third stage of the photocycle, during which the protein partially unfolds as it evolves from the red-shifted to the blue-shifted state. Our aim is to understand what drives the protein to unfold. Specifically, is the isomerization of the

*Correspondence to: Alan E. Mark, Department of Biophysical Chemistry, Groningen Biomolecular Sciences and Biotechnology Institute, Rijsuniversiteit Groningen, Groningen, The Netherlands. E-mail: a.e.mark@chem.rug.nl

Received 2 August 2001; Accepted 15 February 2002

chromophore sufficient to destabilize the protein, or is proton transfer also required?

MATERIALS AND METHODS

MD Simulations

In total, three simulations of PYP under different conditions were performed. Initially, PYP was simulated for 6 ns in the ground state. The starting coordinates for this simulation, denoted as pG, were taken from the high-resolution X-ray structure[4] (entry 2PHY of the PDB). The pG simulation was used as a reference for later work. The second simulation was of the protein in the red-shifted state. This simulation, referred to as pR, was also performed for 6 ns. The starting structure for this simulation was obtained by instantaneously isomerizing the chromphore in the final frame of the ground state simulation (pG). The conformation of the isomerized chromophore was inferred from an X-ray structure of red-shifted state PYP.[6] The X-ray structure of the red-shifted state itself was of insufficient quality to be used as a starting configuration in the simulations, because the structure contains internal strain. In a frame at 2 ns after the start of the second simulation, a proton was manually removed from Glu[46] and added to the chromophore. This modified frame was used as the starting structure in the last 4-ns simulation. This simulation, denoted by pR-H, was performed to investigate the effect of proton transfer on the stability of the protein.

All simulations were performed in a rectangular periodic box, the volume of which was ~168 nm^3. The system contained in total 3617 SPC water molecules,[12] including 92 crystallographic water molecules that were included explicitly. Polar and aromatic hydrogens were added to the protein. In each of the systems simulated, 6 Na^+ ions were added to compensate the net negative charge of the protein. These ions were introduced by replacing the water molecules with the highest electrostatic potential. This was performed in an iterative fashion, that is, after each water molecule was replaced with an ion, the electrostatic potential was recalculated. The final system contained 12663 atoms. Before the pG and pR simulations, the structures were energy minimized for 200 steps by using a steepest-descents algorithm. Subsequently, these structures were simulated for 40 ps with harmonic position restraints on all protein atoms (force constant of 1.0×10^3 kJ $mol^{-1}nm^{-2}$) for an initial equilibration of the water molecules. This equilibration procedure was necessary, especially in the pR simulation, because the instantaneous isomerization procedure could induce strain inside the protein. Neither energy minimization nor any specific equilibration procedure was required in the case of the pR-H simulation, because the transfer of one proton between the two groups induces little strain in the structure and is, in reality, an almost instantaneous process on an MD timescale. All simulations were run at constant temperature and pressure by weak coupling to an external bath[13] (τ_T = 0.1 ps and τ_P = 1.0 ps). The LINCS algorithm[14] was used to constrain bond lengths, allowing a time step of 2 fs. SETTLE[15] was applied to the water molecules. A twin-range cutoff method was used for nonbonded interactions. Lennard-Jones and Coulomb interactions within 1.2 nm were calculated every timestep, whereas Coulomb interactions between 1.2 and 1.8 nm were calculated every 10 steps. All simulations were performed by using the GROMACS simulation package[16] together with the GROMOS96 force field.[17] The generation of additional parameters required to model the chromophore is described below.

TABLE I. Partial Atomic Charges of the Chromophore in the Ground State (pG), Excited State (p*), Deprotonated Red-Shifted State (pR), and Protonated Red-Shifted State (pR-H)†

Atom	pG	p*	pR	pB
Sγ	−0.30	−0.32	−0.20	0.00
C1	0.40	0.15	0.40	0.27
O1	−0.30	−0.43	−0.40	−0.27
C2	−0.58	−0.37	−0.40	−0.20
H2	0.33	0.23	0.10	0.10
C3	0.05	−0.20	0.20	0.00
H3	0.15	0.14	0.10	0.10
C1′	−0.15	−0.10	−0.30	−0.10
C2′	−0.14	−0.10	−0.14	−0.10
H2′	0.14	0.15	0.14	0.10
C6′	−0.14	−0.10	−0.14	−0.10
H6′	0.14	0.15	0.14	0.10
C3′	−0.40	−0.30	−0.34	−0.14
H3′	0.13	0.20	0.14	0.14
C5′	−0.40	−0.30	−0.34	−0.14
H5′	0.13	0.20	0.14	0.14
C4′	0.40	0.40	0.50	0.10
O4′	−0.46	−0.40	−0.60	−0.25
H4′				0.25

†Atom names are as given in Figure 1(a) of the previous article.

Chromophore Force Field

The atomic charges were estimated by fitting to the charge density of the chromophore in vacuo, calculated semiempirically. These computations were performed by using the MOPAC[18] program, with the PM3 Hamiltonian.[19] The ESP charge-fitting procedure[20] was used to derive the atomic charges. The charges were also calculated with the ADF program[21] by using the multipole derived charges procedure.[22] In this procedure, the total charge is distributed per atom in such a way that the partial atomic charges reproduce the atomic multipoles up to the quadrupole. Both approaches yielded similar charge distributions. The average and largest atomic charge variations found were 0.15 e and 0.23 e, respectively. For use in the simulation, the quantum mechanically derived charges were slightly adapted to match similar fragments in the GROMOS96 force field.[17] The final charges are listed in Table I. Dihedral parameters, which model the rotation of the conjugated bonds a, b, c, and d (Fig. 1 of the previous article[2]), were obtained as follows. First, 500,000 chromophore conformations were generated by randomly varying the four dihedral angles. The energy (E^{PM3}) of each of these conformations was then calculated semiem-

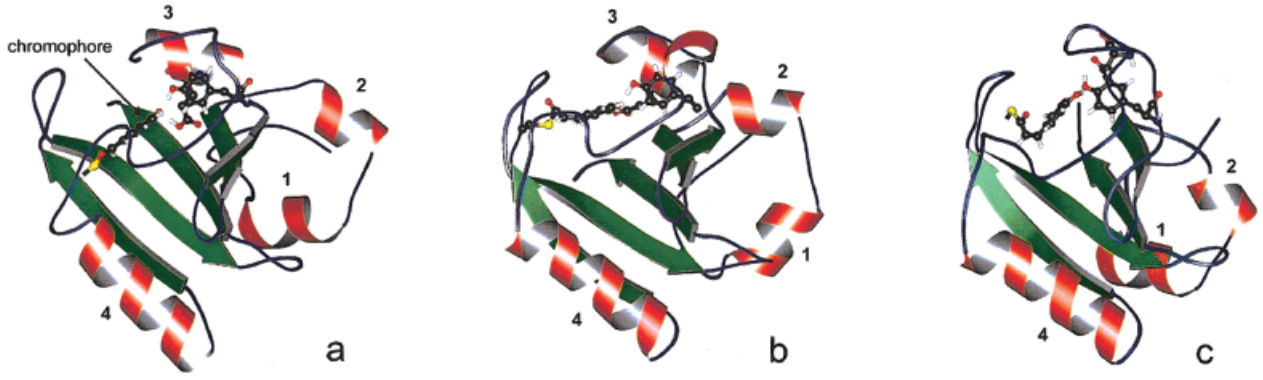

Fig. 1. The time average of the peptide backbone of PYP from molecular dynamics simulations of the protein **a:** Before isomerization of the chromophore (pG). **b:** After isomerization (pR). **c:** After proton transfer from Glu^{46} to the chromophore (pR-H).

pirically. From this energy, the GROMOS96 energy due to all other interactions was subtracted. By performing a multidimensional least-squares fit of four force-field dihedral functions ($V_i(\phi_i) = k_i[1 + \cos(n\phi_i - \phi_{i0})]$, where $i = \{a, b, c, d\}$, $n = 2$ and $\phi_{i0} = \pi$) to the resulting five-dimensional dataset (i.e., $\{a, b, c, d, E\}$ and $E = \Sigma_i V_i$) the required dihedral parameters (k_i) were obtained.

Calculation of the Protein Potentials

During a period of 2 ns, configurations were saved every 10 fs. For each of the 2×10^5 MD frames saved, the proton potentials of both the Tyr^{42} and the Glu^{46} protons were determined. For this purpose, the conformation of the active site, consisting of the chromophore and the side-chains of Tyr^{42} and Glu^{46} was extracted from each frame. The Tyr^{42} proton was then placed at 10 different positions between the hydrogen-bonding donor oxygen atoms ($O\eta$) and the phenolate oxygen atom of the chromophore, after which the same procedure was carried out with the Glu^{46} proton. For each of the resulting $2 \times 2 \times 10^6$ configurations, the active site contribution was calculated at the PM3 level, and to this the classical electrostatic contribution of the environment was added. Cubic spline interpolation was used to complete the potential curves. All protein-active site and solvent-active site interactions were included, by using active site partial charges at every position of the proton. In this way, the complete quantum mechanical response of the active site to the proton position, including polarizability contributions, is incorporated.

RESULTS

Effect of Isomerization

Immediately after the chromophore has isomerized, PYP enters the third stage of the photocycle (Fig. 2 of the previous article[2]). Although the protein is known to undergo large conformational changes during this stage[9] no significant conformational changes were observed in the first 6 ns after isomerization in the simulations. Figure 1 (a, b) shows the PYP backbone conformation averaged over 6 ns for simulations of the ground state (pG, bond *b trans*, Fig. 1 of the previous article[2]) and of the red-shifted state (pR, bond *b cis*, Fig. 1 of the previous article[2]), respectively. The backbone conformations are very similar [the root-mean-square deviation (RMSD) between them is 0.22 nm], indicating that isomerization has had little effect on the overall stability of the protein. Moreover, the hydrogen-bonding network that stabilizes the chromophore in the ground state remains intact after isomerization. As was discussed in the previous article, isomerization is realized by a concerted rotation of all four dihedrals. Overall, the *cis* conformation closely resembles that of the *trans* conformation. There are only minor conformational changes in the chromophore region. However, because the overall length of the chromophore decreases due to the isomerization, the amino acids connected to the chromophore via the thioester linkage on one side and the hydrogen-bonding network on the other, move slightly closer together. Specifically, the disruption of a π-helix (Fig. 1) and the elongation of α-helix 4 by one turn are noted.

As another indicator of stability, the fluctuations of the constituent amino acid residues were considered. Figure 2 shows the time-averaged RMS fluctuations of all amino acids after fitting to a reference structure to remove overall rotational and translational motion. The reference structure was the energy-minimized ground state X-ray structure.[4] The fluctuations are lower in the pR state (thin line in Fig. 2) than in the pG state (thick line). The protein is apparently not destabilized by the isomerization itself.

Proton Transfer

In the ground state, the chromophore is almost completely planar, allowing a near perfect overlap of the p_z orbitals. Consequently, the negative charge on the phenolate oxygen atom is delocalized over the whole chromophore. However, after isomerization, the planarity is lost. This loss is caused by steric hindrance between the carboxylic oxygen atom (O1, Fig. 1 of the previous article[2]) and the phenyl-ring atoms (especially atoms C6′ and H6′). Therefore, in the pR state, the overlap of the atomic p_z orbitals is less and the negative charge is more localized on the phenolate oxygen atom than in the pG state (Table I). Although the increase in charge on this oxygen is small, it strongly increases the probability of a proton transfer from

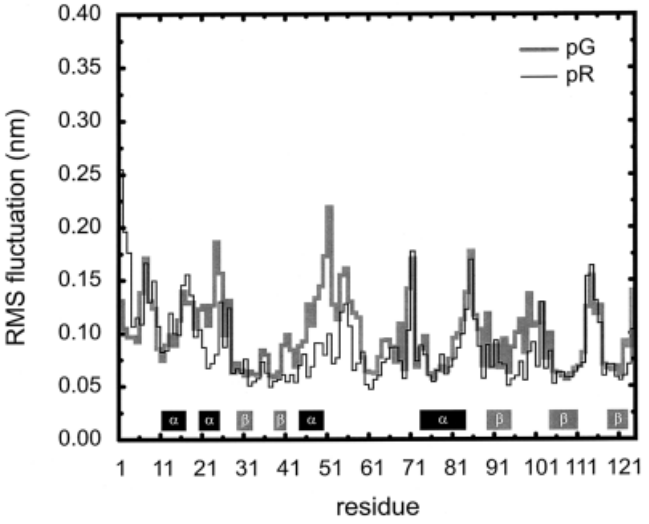

Fig. 2. The time averaged RMS fluctuations of the amino acid residues with respect to the energy-minimized ground state X-ray structure. The thick gray line corresponds to the fluctuations in a 6-ns simulation of the ground state (pG), and the thin black line corresponds to the fluctuations in a 6-ns simulation of the red-shifted state (pR). At the bottom of the figure we indicated the secondary structure type of the residues.

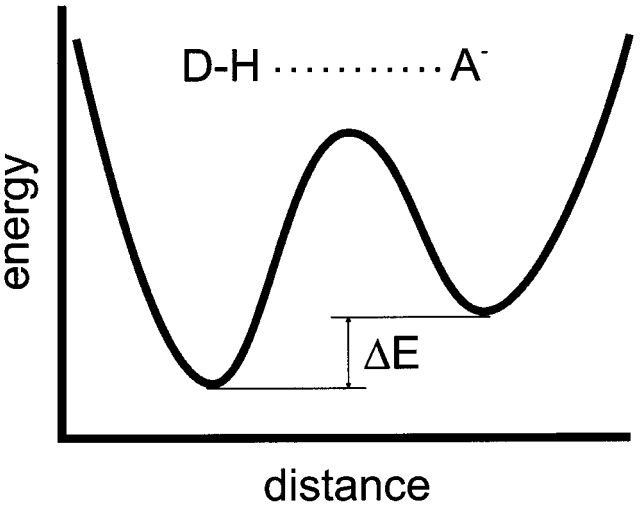

Fig. 3. A schematic potential energy profile for a proton transfer reaction.

one of the hydrogen-bond donor residues (Tyr^{42} and Glu^{46}) to the chromophore.

Two other factors affect the probability of a proton transfer from one of the hydrogen bond donors to the chromophore. The first is the stability of the residue that donates the proton. For example, a proton transfer from the hydroxyl moiety of Thr^{50} is highly unlikely, because the pK_a of this group is very high (it is an aliphatic alcohol group). Second is the nature of the long-range (electrostatic) interactions with the rest of the protein and water. Because the environment is very dynamic, the energy profile of a proton transfer reaction is strongly time dependent. In Fig. 3, such an energy profile is shown schematically. The curve represents the potential energy of the system as a proton migrates from a hydrogen bond donor to an acceptor. Typically, such a curve consists of two local minima, representing a covalent bond to the donor and acceptor, respectively, separated by a barrier. The difference in energy between these minima (ΔE in Fig. 3) determines the equilibrium constant of the proton transfer reaction. The height of the barrier (E^{TST}) controls the rate at which the system approaches equilibrium. Because both the energy difference between the minima and the height of the barrier depend on the environment, spontaneous fluctuations in the environment can drive a proton from one residue to the other.

In the simulations, the protein remains stable after isomerization. The phenolate moiety of the chromophore is not exposed to solvent. Therefore, only intramolecular proton transfer is possible. The candidates for donating a proton to the chromophore are the sidechains of Tyr^{42} and Glu^{46} (Fig. 1 of the previous article[2]). To determine whether a proton transfer from one of these residues is more likely in the red-shifted state than in the ground state, the time evolution of the corresponding proton potential energy curves was monitored in both the pG and pR simulations. The time evolutions of the energy splitting $\Delta E(t)$ for the transferable protons of Tyr^{42} and Glu^{46} in the ground state and in the red-shifted state are depicted in Figure 4. The splitting is defined as the difference in total potential energy before and after proton transfer, calculated by using the PM3 Hamiltonian[19] (see Materials and Methods). A positive splitting means that a proton transfer is energetically unfavorable. The energy differences for both protons are always around 130 kJ/mole in the ground state [Fig. 4(a) and (b)]. Thus, a proton transfer from one of the hydrogen bond donors to the chromophore is very unlikely in the ground state. However, after isomerization there are periods during which the splittings become negative [Fig. 4(c) and (d)]. During these periods, a proton transfer from Tyr^{42} as well as from Glu^{46} would be energetically favorable. However, because the splitting of the Glu^{46} proton is the more negative in those periods [Fig. 4(d)], it is most likely that this proton is the one transferred.

At 2 ns in the pR simulation, the energy splitting of the Glu^{46} proton is most favorable for a transfer (note from Fig. 4 that the monitoring period started 1 ns after the start of the pR simulation). Therefore, at this time point, the proton was manually transferred from the glutamic acid to the chromophore, and a new simulation, named pR-H, was initiated. Immediately after the start of this simulation, the hydrogen-bonding network that stabilized the deprotonated chromophore in the previous simulations was lost. Figure 5 shows the distance between the donor and acceptor oxygen atoms involved in that network plotted versus time, both before [Fig. 5(a)–(f)] and after [Fig. 5(g)–(l)] the proton transfer. At the start of the pR-H simulation, the distances between the protonated chromophore and residues Glu^{46} and Tyr^{42} rapidly increase. Moreover, the distances show greater fluctuations than the previous simulation (Fig. 5, upper panels). This indi-

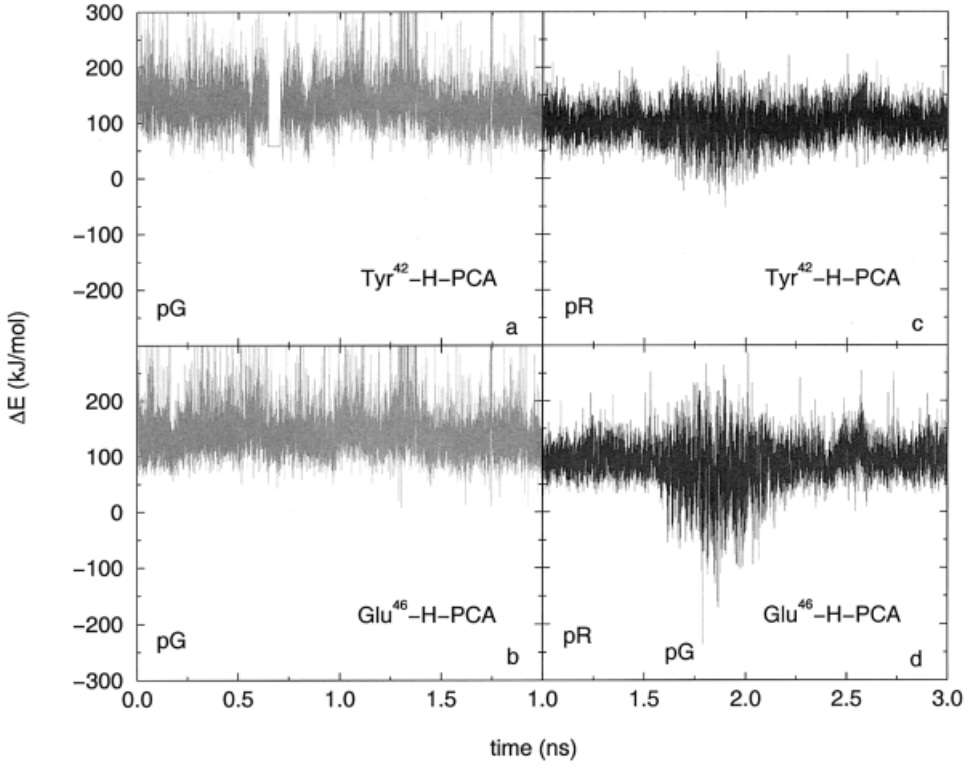

Fig. 4. The energy splitting defined as the difference between the minima of the two proton wells (ΔE in Figure 3), as a function of time: **a:** The splitting for the Tyr^{42} proton in pG; **b:** The splitting for the Glu^{46} proton in pG; **c,d:** The splittings in pR for Tyr^{42} and Glu^{46}, respectively.

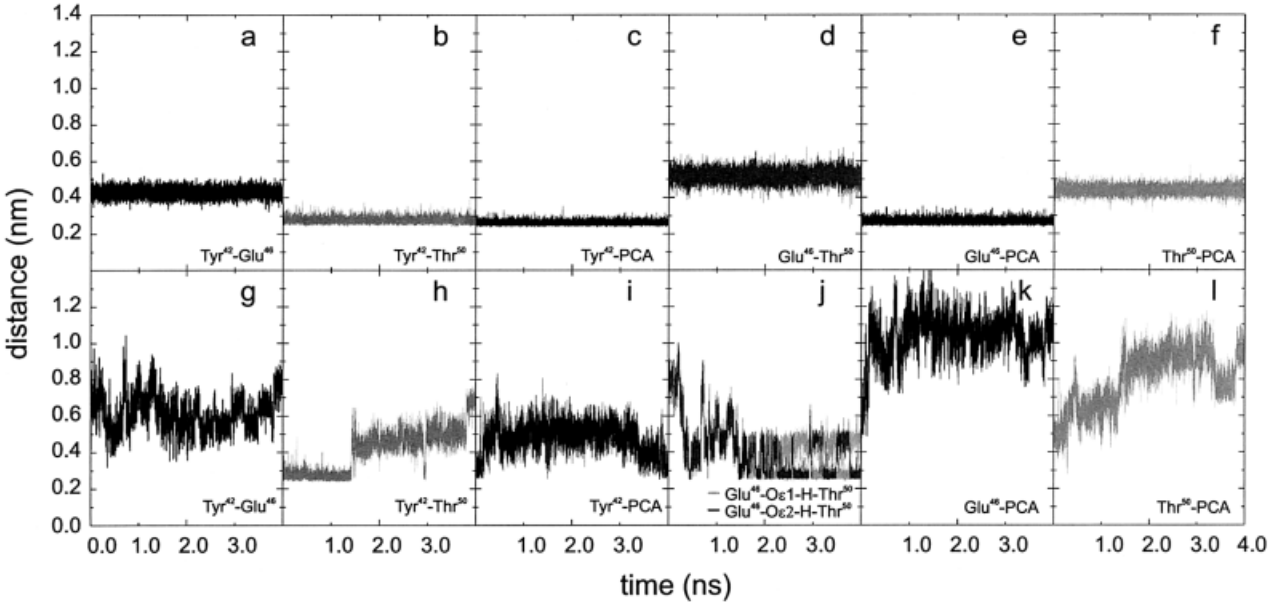

Fig. 5. The distances between the hydrogen bond donating oxygen atoms and the accepting oxygen atoms. The upper panels show the distances before proton transfer, and the lower panels show the distances after a proton transfer from the Glu^{46} side-chain to the phenolate group of the chromophore.

cates that the hydrogen-bonding network has collapsed. An important consequence of this rapid collapse is that the proton transfer from Glu^{46} to the chromophore is effectively irreversible. After the transfer, the chromophore is a possible hydrogen bond donor. In Figure 5(i), we see that after 3.5 ns, the chromophore does indeed donate a hydrogen bond to the phenol moiety of Tyr^{42}. This hydrogen bond remains stable throughout the rest of the simulation.

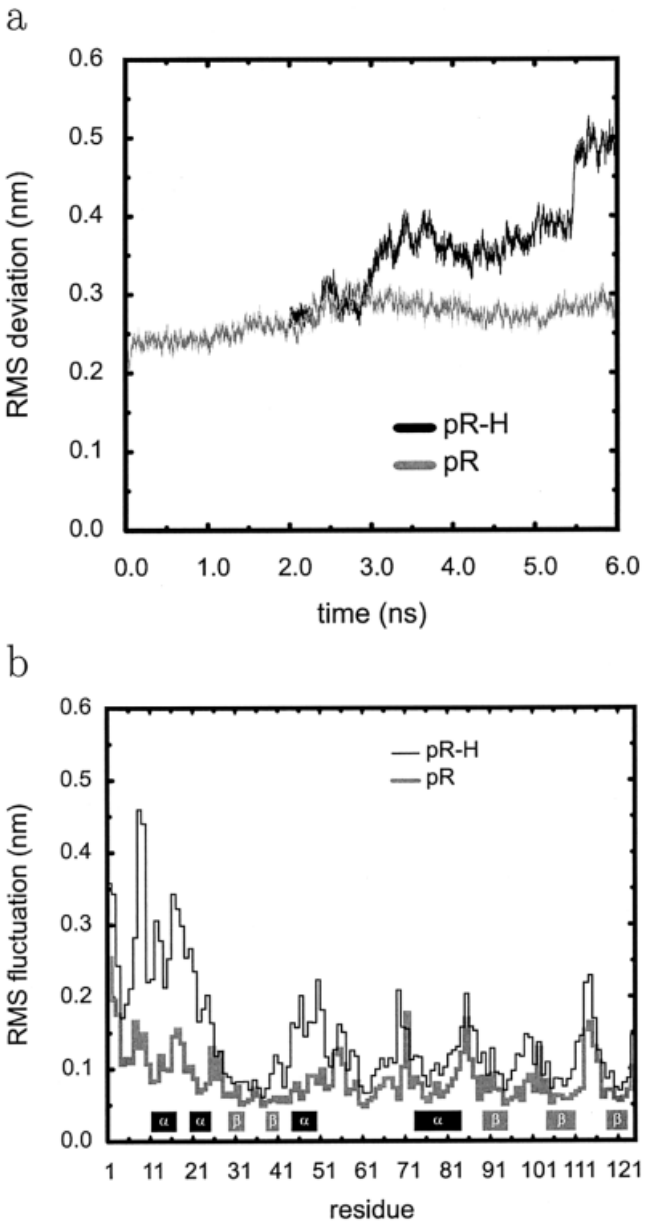

Fig. 6. **a:** The evolution of RMSD for the energy-minimized X-ray ground state structure. The thick gray line corresponds to the RMSD of the backbone before proton transfer between the Glu^{46} side-chain and the phenolate group of the chromophore. The thin black line corresponds to the RMSD after proton transfer. **b:** The time-averaged RMS fluctuation per residue, both before (thick gray, pR) and after the proton transfer (thin black, pR-H). At the bottom of this plot we indicated the secondary structure type of the residues.

The negatively charged carboxylate group of Glu^{46} is partly stabilized by a hydrogen bond with the Thr^{50} side-chain. As Figure 5(j) shows, this hydrogen bond interchanges rapidly between the two oxygen atoms of the Glu^{46} side-chain.

The transfer of the proton has an effect on the stability of the protein. Figure 6 shows the RMSD of the protein backbone before and after the proton transfer. In Figure 6(a), the RMSD of all backbone atoms is plotted versus time. Figure 6(b) shows the time-averaged RMSD per residue. The reference structure in both calculations was the energy-minimized ground state X-ray structure,[4] as before (see Fig. 2). In Figure 6(a), one sees that the RMSD of the pR-H simulation rises to twice that of the pR simulation in <4 ns. Moreover, as is evident from Figure 6(b), the time-averaged fluctuations for all residues are larger after the transfer of the proton. The largest increase is observed in the residues of the N-terminal domain. The most prominent structural change, however, was observed in a region close to the chromophore, where an α-helix (α-helix 3, Fig. 1) is completely lost. This can be seen from Figure 1(c), which shows the time-averaged backbone in the pR-H simulation. Although this structure looks quite similar to the structures of the pG and pR simulations, one can clearly see that α-helix 3 is no longer present in the averaged pR-H structure. This indicates that the destabilization is not restricted to the N-terminal domain of the protein.

DISCUSSION

The light-induced *trans*-to-*cis* isomerization of the chromophore in the second stage of the PYP photocycle results in a contraction of around 0.05 nm in the overall length of the chromophore (as measured by the distance from the Cys^{69} Sγ atom to the phenolate O4′ atom [Fig. 1 of the previous article[2]]. In the *cis* conformation, steric repulsion between the carboxylic oxygen atom (O1, Fig. 1 of the previous article[2]) and two phenyl ring atoms (C6′ and H6′) prevents the chromophore from being planar. The overall conjugation via the overlap of atomic p_z orbitals is decreased by the loss of planarity, and this results in less effective delocalization of the chromophore's negative charge. One consequence of this is an accumulation of negative charge on the phenolate oxygen atom (O4′, Fig. 1 of the previous article[2]). This electrostatically reinforces the hydrogen-bonding network between the chromophore phenolate oxygen atom and the hydroxyl groups of Tyr^{42} and Glu^{46}. Because of this electrostatic reinforcement, the shortening of the chromophore is not accompanied by a collapse of the hydrogen bonding network but, rather, by a small contraction of two protein domains that are connected through the chromophore. Moreover, the reinforcement of the hydrogen-bonding network argues against the possibility of a proton transfer from or via a water molecule, because the chromophore remains protected from solvent.

The structural changes caused by the contraction of the chromophore are probably too small to result in signal transduction. Furthermore, the slightly contracted protein with an isomerized chromophore appears to be more stable than the uncontracted ground state protein in the simulations. This finding is in contrast with that of van Aalten et al.,[23] who attributed the large conformational changes that take place after the isomerization to the isomerization itself. However, their isomerization procedure was different from that used in this study. Aalten et al. allowed bond *b* (Fig. 1 of the previous article[2] to rotate freely during a short time interval. However, as was shown in the previ-

ous article, the isomerization involves concerted rotations of all four dihedrals, and, therefore, allowing only bond *b* to rotate will not lead to an appropriate pR conformation.

The isomerization of the chromophore with the accompanying localization of negative charge on the phenolate oxygen does, however, open the way for the transfer of a proton from the carboxylic acid side-chain of Glu^{46} to the phenolate group of the chromophore. Before isomerization, this proton transfer is strongly endothermic and very unlikely to occur in the ground state. After isomerization, fluctuations in the protein are sufficient to make the transfer exothermic, and during such fluctuations, proton transfer is likely to occur.

The immediate effect of the proton transfer is the collapse of the hydrogen-bonding network, making the transfer effectively irreversible. After the transfer, the chromophore is no longer negatively charged, and the electrostatic contribution to the hydrogen bond formed between the chromophore and Tyr^{42} (Fig. 1 of the previous article[2]) is decreased. Moreover, because the negative charge on the glutamate residue is delocalized over two oxygen atoms and the connecting carbon atom, the hydrogen bond between the chromophore and this residue is also weakened. The strain introduced by the contraction of the chromophore after isomerization is now sufficient to disrupt the hydrogen bonds. The bridge the chromophore formed between two domains of the protein is also broken and, as a consequence, this part of the protein is destabilized.

Another consequence of the transfer is that the negative charge inside the hydrophobic chromophore pocket becomes even more localized. Before the transfer, this charge is delocalized over a large part of the chromophore. After the transfer, the charge is spatially restricted to the carboxylate moiety of the glutamate sidechain. Strongly localized charges buried inside hydrophobic pockets are, in general, energetically unfavorable, and this charge redistribution probably also helps to initiate the unfolding of PYP. The N-terminal domain of the protein is primarily affected and shows the largest changes in the simulation, in line with recent experimental observations.[24] The N-terminal domain contains several negatively charged glutamate (n = 3) and aspartate (n = 2) residues. It is possible that electrostatic repulsion between the Glu^{46} side-chain and the N-terminal region may also play a role in driving the conformational changes.

The rate at which pR is converted to the next intermediate pB depends on both the rate of proton transfer and the rate of unfolding. The rate of proton transfer is determined by the frequency of protein fluctuations that make the transfer possible. The transfer itself is probably not rate limiting. The experimentally observed interconversion rate of pR to pB has been analyzed by different authors in terms of two to four exponential decay processes with time constants in the range of milliseconds.[6,25] Clearly, because we only simulated 4.0 ns of a process, which in fact takes several microseconds, we cannot draw definite conclusions about the later stages in the evolution toward the blue-shifted state. However, even in this short period, significant changes were observed in the N-terminal domain of the protein as well as the disappearance of one helix, which could represent initial events in the unfolding process.

One potential limitation in our approach is that the excess energy that enters the system during the photon absorption was not taken into account. This energy is dissipated into the chromophore and its surroundings during and after the isomerization. Because the amount of energy carried by the photon is large (~300 kJ/mol), the apparent stability found after isomerization may be an artifact. The increase of kinetic energy in the region of the chromophore might itself lead to some unfolding. However, in the free isomerization simulations (see previous article), the excess energy was, to a first approximation, accounted for, yet no destabilization during or after the isomerization of the chromophore was observed. In general, temperature gradients within proteins dissipate very rapidly, and as soon as the excess energy is distributed over hundred atoms, the effects are of thermal magnitude. For these reasons, we believe that the energy that enters the system via photon absorption has at most a minor effect on the red-shifted state.

CONCLUSIONS

The simulation studies presented here suggest that the light-induced isomerization of the chromophore alone does not destabilize the protein nor lead to unfolding. It does, however, enhance the probability of a proton transfer from the hydroxyl oxygen atom of a glutamic acid residue (Glu^{46}) to the phenolate oxygen atom of the isomerized chromophore. From the simulations, we propose that it is the redistribution of charge and the breaking of hydrogen-bonding interactions associated with the proton transfer that results in partial unfolding of the protein and eventually signal transduction.

REFERENCES

1. Hellingwerf K, Crielaard W, de Mattos, MJT, Hoff W, Kort R, Verhamma D, Avignone-Rossa C. Current topics in signal transduction in bacteria. Antonie van Leeuwenhoek 1998;74:211–227.
2. Groenhof G, Lensink MF, Berendsen HJC, Suijders JG, Mark AE. Signal transduction in the photoactive yellow protein. I. Photon absorption and the isomerization of the chromophore. Proteins 2002;48:202–211.
3. Baca M, Borgstahl G, Boissinot M, Burke P, Williams D, Slater K, Getzoff E. Complete chemical structure of photoactive yellow protein: novel thioester-linked 4-hydroxyxinnamyl chromophore and photocycle chemistry. Biochemistry 1994;33:14369–14377.
4. Borgstahl GEO, Williams DR, Getzoff ED. 1.4 Å structure of photoactive yellow protein, a cytosolic photoreceptor: unusual fold, active site and chromophore. Biochemistry 1995;34:6278–6287.
5. Hendriks J, Hoff WD, Crielaard W, Hellingwerf KJ. Protonation/deprotonation reactions triggered by photoactivation of photoactive yellow protein from *ectothiorodospira halophila*. J Biol Chem 1999;274:17655–17660.
6. Perman B, Šrajer V, Ren Z, Teng TY, Pradervand C, Ursby T, Bourgeois D, Schotte F, Wulff M, Kort R, Hellingwerf KJ, Moffat K. Energy transduction on the nanosecond time scale: early structural events in a xanthopsin photocycle. Science 1998;279:1946–1950.
7. Xie A, Hoff WD, Kroon AR, Hellingwerf KJ. Glu46 donates a proton to the 4-hydroxycinnamate anion chromophore during the photocycle of photoactive yellow protein. Biochemistry 1996;35:14671–14677.

8. Genick UK, Borgstahl GE, Ng K, Ren Z, Pradervand C, Burke PM, Šrajer V, Teng TY, Schildkamp W, McRee DE, Moffat K, Getzoff ED. Structure of a protein photocycle intermediate by millisecond time-resolved crystallography. Science 1997;275:1471–1475.
9. Rubingstenn G, Vuister GW, Mulder FAA, Düx PE, Boelens R, Hellingwerf KJ, Kaptein R. Structural and dynamic changes of photoactive yellow protein during its photocycle in solution. Nat Struct Biol 1998;5:568–570.
10. Allen MP, Tildesley DJ. Computer simulations of liquids. Oxford: Oxford Science Publications; 1987.
11. Frenkel D, Smit B. Understanding molecular simulations: from algorithms to applications. New York: Academic Press; 1996.
12. Berendsen HJC, Postma JPM, van Gunsteren WF, Hermans J. Interaction models for water in relation to protein hydration. In: Pullman B, editors Intermolecular forces. Dordrecht: D. Reidel Publishing Company; 1981. p 331–342.
13. Berendsen HJC, Postma JPM, van Gunsteren WF, DiNola A, Haak JR. Molecular dynamics with coupling to an external bath. J Chem Phys 1984;81:3684–3690.
14. Hess B, Bekker H, Berendsen HJC, Fraaije JGEM. LINCS: a linear constraint solver for molecular simulations. J Comp Chem 1997;18:1463–1472.
15. Miyamoto S, Kollman PA. SETTLE: an analytical version of the SHAKE and RATTLE algorithms for rigid water models. J Comp Chem 1992;13:952–962.
16. van der Spoel D, Hess B, Feenstra KA, Lindahl E, Berendsen HJC. GROMACS user manual version 2.0. Nijenborgh 4, 9747 AG Groningen, The Netherlands. Internet: http://md.chem.rug.nl/~gmx 1999.
17. van Gunsteren WF, Billeter SR, Eising AA, Hünenberger PH, Krüger P, Mark AE, Scott WRP, Tironi IG. Biomolecular simulation: GROMOS96 manual and user guide. BIOMOS b.v. Zürich, Groningen 1996.
18. Stewart JJP. Mopac version 2000. Tokyo, Japan: Fujitsu Limited; 1999.
19. Stewart JJP. Optimization of parameters for semiempirical methods I. methods. J Comp Chem 1989;10:209–220.
20. Besler BH, Merz KM Jr, Kollman PA. Atomic charges derived from semiempirical methods. J Comp Chem 1990;11:431–439.
21. te Velde G, Bickelhaupt FM, Baerends EJ, van Gisbergen SJA, Guerra CF, Snijders JG. Chemistry with adf. J Comp Chem 2001;22:931–967.
22. Swart M, van Duijnen PT, Snijders JG. A charge analysis derived from an atomic multipole expansion. J Comp Chem 2000;22:79–88.
23. van Aalten DMF, Hoff WD, Findlay JB, Crielaard W, Hellingwerf KJ. Concerted motions in the photoactive yellow protein. Protein Eng 1998;11:873–879.
24. Craven CJ, Derix NM, Hendriks J, Boelens R, Hellingwerf KJ, Kaptein R. Probing the nature of the blue-shifted intermediate of photoactive yellow protein in solution by nmr: hydrogen-deuterium exchange data and ph studies. Biochemistry 2000;39:14392–14399.
25. Brudler R, Rammelsberg R, Woo T, Getzoff E, Gerwert K. Structure of the i_1 early intermediate of photoactive yellow protein by ftir. Nat Struct Biol 2001;8:265–270.